ISSN 2517-7516, Membranes and Membrane Technologies, 2024, Vol. 6, No. 2, pp. 120–131. © Pleiades Publishing, Ltd., 2024.

Transport and Structural Characteristics of Heterogeneous Ion-Exchange Membranes with Varied Dispersity of the Ion Exchanger

V. I. Vasil'eva[a], E. E. Meshcheryakova[b], O. I. Chernyshova[b], M. A. Brovkina[b], I. V. Falina[b, *], E. M. Akberova[a], and S. V. Dobryden'[a]

[a] *Voronezh State University, Voronezh, 394018 Russia*

[b] *Kuban State University, Krasnodar, 350040 Russia*

**e-mail: Irina_falina@mail.ru*

Received October 19, 2023; revised November 28, 2023; accepted December 7, 2023

Abstract—The structural and transport (conductivity, diffusion permeability) properties of cation- and anion-exchange membranes with varied dispersity of ion-exchange resin particles are studied in the work. Experimental MK-40 cation-exchange and MA-41 anion-exchange membranes with variable particle size of the ion-exchange resin of <20 to <71 μm were manufactured at LLC IE Shchekinoazot (Russia). A comparative analysis of the structural characteristics of the membranes by SEM reveals the anisotropy in the properties of the surface and section. The internal phase of the membrane is characterized by high values of the fraction and sizes of the ion exchanger and macroporosity. A comparison of the concentration dependences of the specific conductivity and diffusion permeability of the experimental membranes is performed. The analysis of the values of the model transport-structural parameters shows that an increase in the conductivity of the gel phase from 0.39 up to 0.47 S/m and from 0.15 up to 0.26 S/m for cation- and anion-exchange membranes, respectively, as well as redistribution of current transfer paths in the membrane are observed in the case of a decrease in the particle size of the ion exchanger. An increase in the contribution from transfer of the internal equilibrium solution along the channel is revealed; here, the transfer numbers of counterions slightly change. Information about the changes in the structure of the transport channels in membranes with different particle sizes of the ion exchanger obtained based on the analysis of the model parameters is consistent with the data of independent studies of the morphology of their surface and section by SEM.

Keywords: ion-exchange membrane, particle size of ion exchanger, conductivity, diffusion permeability, transport-structural parameters

DOI: 10.1134/S2517751624020082

INTRODUCTION

Currently, heterogeneous ion-exchange membranes find wide application in electromembrane processes of concentration and desalination. Because of this, obtaining heterogeneous ion-exchange membranes with improved properties is currently in demand. Effective ways of modification are profiling of the surface and a decrease in the thickness as well as variation of the concentration of ion-exchange resins in the composition of ion-exchange membranes. Modifying membranes by changing the ion-exchanger/inert binding agent volume ratio [1, 2], a compromise between the electrochemical and mechanical properties can be achieved to obtain a membrane with improved properties. The interest in such materials is determined by the possibility of controlling the onset and development of electroconvection to intensify the mass transport in overlimiting current modes [3–5] as a result of changing the geometric and electrical nonuniformity of the membrane surface.

The effect of the ratio of the ion-exchange resin and polymer binding agent in membranes obtained by casting from a solution of polymers [6–9] on their electrotransport properties has been widely studied. Currently, increasing attention is paid not only to the concentration but also to the dispersity of the ion exchanger particles in the composition of heterogeneous ion-exchange membranes. Currently produced ion-exchange membranes contain particles with a wide size distribution. At the same time, heterogeneous cation-exchange membranes have been studied in [10], in which charged polystyrene microspheres were used as ion exchangers. The microspheres had a significantly smaller particle size (about 10 μm) and a narrower size distribution than known commercial powders of resins (about 30 μm). This made it possible to decrease the concentration of an ion exchanger in a membrane without sacrificing its high electrical con-

ductivity. Comparing the current–voltage curves of Ralex (Mega a.s., Czech Republic) and MK-40 and MA-41 (LLC IE Shchekinoazot, Russia) heterogeneous membranes that differed by the dispersity of the ion exchanger particles showed that the fraction of the active surface in Ralex membranes with a smaller particle size is twofold higher [11]. Such properties of the surface lead to a decrease in the length of the plateau and an increase in the value of the limiting current in comparison with MK-40 and MA-41 membranes.

The simultaneous action of both the particle size and concentration of the ion-exchange resin on the properties of experimental cation- and anion-exchange heterogeneous membranes has been studied in [12, 13]. Membranes based on polyvinylchloride as a binding agent and a powder of an ion-exchange resin as a polyelectrolyte obtained by casting from a solution have been studied in the works. The authors have shown that the specific conductivity and exchange capacity of the membranes grow with the increase in the concentration of the resin in them; however, the mechanical strength of the samples deteriorated. In addition, at the same load of the cation exchanger and thickness of membranes, an increase in the specific conductivity and exchange capacity was observed with decreasing particle size of the resin.

The variation of the dispersity of the ion-exchange resin particles in commercially available heterogeneous membranes conventionally obtained under factory conditions by rolling followed by pressing and investigation of their transport properties are especially relevant. The aim of this work is the investigation of the effect of the dispersity of the ion-exchange resin in the composition of heterogeneous cation- and anion-exchange membranes on their physicochemical properties and transport-structural parameters. The tasks of the work included the measurement of the physicochemical characteristics of the heterogeneous membranes under study and investigation of the structural properties of their surface and section, acquisition of the concentration dependences of specific conductivity and diffusion permeability, and calculation and analysis of the transport-structural parameters of the microheterogeneous and extended three-wire models for the membranes under study with varied dispersity of the ion exchanger.

EXPERIMENTAL

Study Objects

Experimental MK-40 cation- and MA-41 anion-exchange membranes (LLC IE Shchekinoazot, Russia) with variable dispersity of the ion-exchange resin particles of 56–71 to <20 μm were used as the study objects. MK-40 and MA-41 heterogeneous membranes are composites of an ion exchanger with polyethylene and reinforcing fibers made of Capron. The weight fraction of a strongly acidic KU-2-8 cation exchanger (TOKEM Trading Company LLC, Kemerovo) in the composition of an MK-40 membrane is 65%. An MA-41 membrane contains 60 wt % strongly acidic AV-17-8 anion-exchange resin (TOKEM Trading Company LLC, Kemerovo). The weight fraction of the ion-exchange resin characterizes the ratio of the weight of the weighed amount of a dry ion-exchange resin to the weight of a mixture of polyethylene and a resin, from which the membrane is made. The corresponding ion-exchange resin/polyethylene ratios are used by LLC IE Shchekinoazot in the technology process of production of commercial MK-40 and MA-41 membranes. Sulfo groups are the fixed groups of a KU-2 cation exchanger. An AV-17 anion exchanger contains one type of ionogenic groups—quaternary ammonium bases. Linear polyethylene of the L461N00 brand (LLC Khemiks, Kirishi) is used as an inert binding agent in the membranes, while an Excelsior Capron mesh art. 56314 (CJSC Rakhmanovskii shelkovyi kombinat, Pavlovsky Posad) acts as a reinforcing cloth. In the process of production of the membranes, the initial ion-exchange resins were dried and ground in an ejector jet mill of the 3SV-600 type. The particle sizes were determined by the value of the residue of a dry ion-exchange resin on sieves with the corresponding width of the apertures in μm using a sieve analyzer consisting of a vibration motor and mounted on it tray and a set of five sieves (with the diameter of the sieve meshes of 71, 56, 40, 32, 20 μm). A membrane blank was obtained by rolling of a mixture of polyethylene and an ion-exchange resin which was further reinforced with the cloth and pressed.

Prior to the study, the membranes were subjected to salt pretreatment [14] followed by transformation to the H^+ or OH^- form by the treatment with HCl or NaOH. Then the samples were washed with distilled water with the control of the resistance of water over the membrane.

Procedures for the Determination of the Physicochemical and Transport Characteristics of the Membranes

The exchange capacity Q, mmol/g, was determined for the samples of cation- and anion-exchange membranes in the H^+ and OH^- forms based on the results of determination of the decline in the concentration of an alkali or an acid from a solution after contact with the membrane by acid–base titration. The water content W, %, was determined by air heat drying of the samples of the membranes in the Na^+ and Cl^- form at 100°C to a constant weight. The value of the water content was calculated as a ratio of the weight loss of a sample in the process of drying to its weight in the swelled state. The specific water content n_m, mol of H_2O/mol of fixed groups, was calculated based on the data on the exchange capacity and water content of the membranes. The density of the membranes was determined by hydrostatic weighing. The values of the

Table 1. Structural characteristics of the surface of the initially swelled samples of MK-40 and MA-41 membranes with different particle sizes of the ion-exchange resin

Membrane	Particle sizes, μm	S, %	P, %	$\bar{r}$, μm
MK-40	<20	20.9 ± 1.4	4.7 ± 0.8	1.8 ± 0.3
	56–71	17.7 ± 1.7	4.4 ± 1.7	2.2 ± 0.2
MA-41	<20	16 ± 3	3.8 ± 0.5	1.7 ± 0.3
	56–71	13 ± 7	2.4 ± 0.7	2.0 ± 0.2

physicochemical parameters of the membranes are presented in Table 1.

The specific conductivity of the ion-exchange membranes in solutions of sodium chloride was found from the data on their resistance measured on the alternating current. Prior to the measurement, the membrane was equilibrated with a solution of sodium chloride with a set concentration. The resistance was measured using a mercury contact call [15]. The high-frequency cutoff onto the axis of active resistances in the impedance spectrum was taken as the resistance of the membranes. The resistance was measured using a PGSTAT P-45X potentiostat-galvanostat. The specific conductivity of the membrane κ, S/m, was calculated by the formula

$$\kappa = \frac{l}{RS_m}, \quad (1)$$

where l is the thickness of the membrane, m; R is the measured resistance, Ω; and S_m is the working area of the membrane, m^2.

To measure the diffusion permeability of the membranes in a free-standing state, a two-compartment cell was used. One of the compartments equipped with platinized platinum electrodes for recording the resistance of the solution was filled with distilled water, and the second, with a solution of sodium chloride with a set concentration. The solutions at both sides of the membrane were stirred with a stirrer at a speed of 120 rpm to eliminate the effect of the diffusion layers at the membrane/solution boundaries. The resistance of the solution in the compartment with distilled water was recorded using an E 7-21 immitance meter (NPI MNIPI, Minsk, Belarus). The diffusion flux of the electrolyte through the membrane in the steady state j, mol m^{-2} s^{-1}, and integral coefficient of diffusion permeability P, m^2/s, were calculated by the formulae

$$j = \frac{VdC}{S_m dt}, \quad (2)$$

$$P = \frac{jl}{C_0}, \quad (3)$$

where V is the volume of the electrolyte, m^3; $\frac{dC}{dt}$ is the change in the concentration in the compartment with water over time, mol m^{-3} s^{-1}; and C_0 is the concentration of the electrolyte, mol/m^3.

The transport characteristics were measured at least three times each at 25°C. The value of the relative systematic error of determination of diffusion permeability and specific conductivity of the membrane did not exceed 5%. Prior to the study, the samples were equilibrated with solutions of sodium chloride with a set concentration. The thickness of the samples was measured in ten points of the sample using an Inforce 06-11-45 digital micrometer with an accuracy of no less than 0.003 mm.

Calculation of the Transport-Structural Parameters

The approaches of microheterogeneous [16] and extended three-wire [17] models make it possible to calculate the transport-structural parameters of membranes based on the concentration dependences of their transport characteristics. These approaches are based on the representation of an ion-exchange membrane as a microheterogeneous material and a theory of generalized conductivity of structurally inhomogeneous media. According to the microheterogeneous model, all the elements of an ion-exchange membrane are grouped into two pseudophases with different types of conductivity: a gel phase and an intergel solution phase (Fig. 1) which are characterized by the volume fractions (f_1 and f_2, respectively) and mutual arrangement of the phases—a parameter α [18]. The gel and intergel solution phases possess electrically conductive (specific conductivity of the gel κ_{iso} and solution κ_{sol}) and diffusion characteristics (the Gnusin complex parameter G and coefficient of diffusion of the electrolyte D for the gel and solution, respectively). The specified parameters can be calculated based on the concentration dependences of specific conductivity and diffusion permeability.

According to the extended three-wire model [16], current passes through an ion-exchange material along three parallel channels: successively through the ion exchanger and the solution, through the ion exchanger only, and through the solution only (a, b, c are the geometric parameters characterizing the fractions of the current passing through a mixed channel with successive alternation of the ion exchanger and solution phases, through the ion exchanger only, and

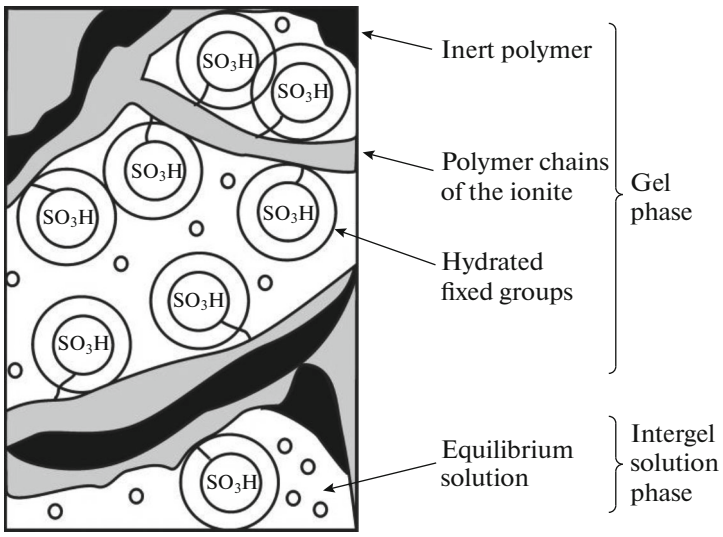

Fig. 1. Microheterogeneous structure of a heterogeneous sulfo cation-exchange membrane.

through the solution only ($a + b + c = 1$); d, e are the fractions of the solution and ion exchanger in the mixed channel ($d + e = 1$)). The extended three-wire model makes it possible to find the structural (f_1, α) and geometric (a, b, c, d, e) parameters based on the concentration dependence of the electrical conductivity of the ion-exchange material alone. On an assumption that the current in channels a and b is transferred by counterions only, and in channel c, by counter- and coions, an equation for the calculation of the transfer number of the counterion in the membrane $\overline{t_+}$ can be obtained if the fraction of current passing along the solution channel (parameter c) is known:

$$\overline{t_+} = 1 - t_- \frac{c}{K_m}, \quad (4)$$

where t_- is the transfer number of coions in the solution and K_m is the relative electrical conductivity of the membrane ($K_m = \kappa_m/\kappa_{sol}$). This assumption is true for diluted and moderately concentrated solutions, where the Donnan sorption of the electrolyte can be neglected.

Study of the Surface and Section of the Membranes by Scanning Electron Microscopy

The electron microscopic recording of the surface and section of the experimental samples of the membranes was performed in their initially swelled state in a low-vacuum mode with the use of backscattered (reflected) electrons at an accelerating potential of 20 kV on a JSM-6510 microscope (Japan). The main factor affecting the number of reflected electrons (the signal of backscattered electrons) is the elemental composition of the region of detection [19]. The areas of the surface under analysis containing heavy atoms with a higher ordinal number give light regions in the image due to the reflection of a higher number of electrons at a smaller depth in the sample and with lower energy losses. Therefore, the light grey regions correspond to the phase of the ion exchanger, the ionogenic groups of which contain sulfur, oxygen, and nitrogen atoms; the dark grey color corresponds to the phase of polyethylene, the composition of which includes carbon atoms. In the mode of backscattered electrons, the deep pores and structural defects are visualized by black color due to the absorption of the incident beam electrons in them and significant energy losses upon their movement to the surface. The proposed approach to the interpretation and processing of the SEM images of the surface and section of ion-exchange membranes was multiply applied for the quantitative assessment of their structure [1, 11, 20].

The quantitative assessment of the fraction of the ion-exchange material and pore composition on the surface and in the section of the membranes was performed with the use of a customized software complex [20], in which methods of digital processing of electron microscopic photographs of membranes are implemented. This made it possible to carry out an automated analysis of the morphology of the surface and section. The following structural parameters were determined: fraction of the surface occupied by the ion exchanger S, %; macroporosity P, %; and radius of the ion exchanger R, μm, or macropore r, μm. The fraction of the ion-exchange material was determined as the fraction of the surface area occupied by the ion exchanger $S = \left(\sum S_i/S\right) \times 100\%$, where $\sum S_i$ is the total area of the ion-exchange regions of the surface and S is the area of the scanned region. The macroporosity of the surface and section of the membranes was determined in a similar manner. The effective radius of the round-shaped region modeled by the program which is equivalent in the area to the real area of the

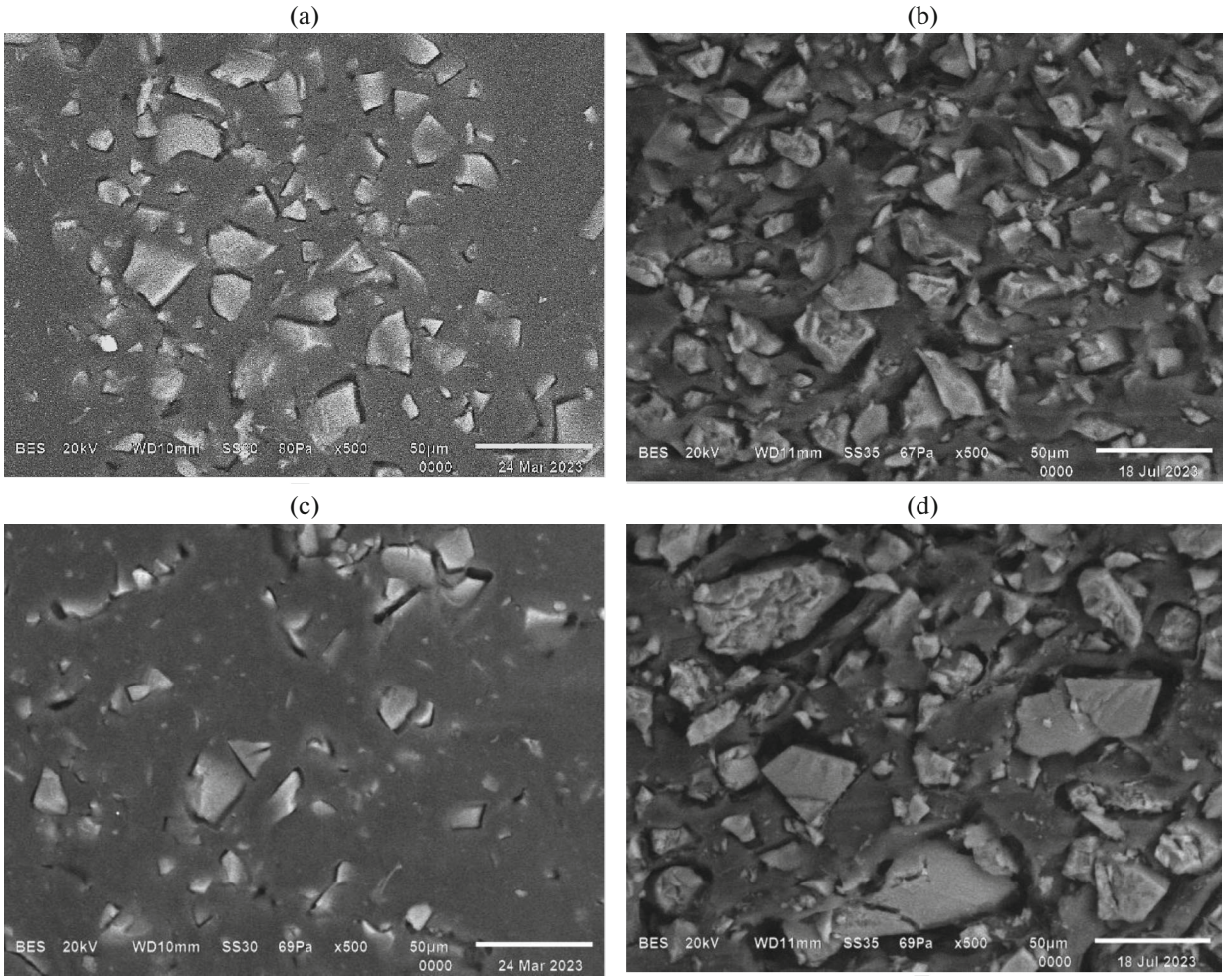

Fig. 2. SEM images of the (a, c) surface and (b, d) section of the initially swelled samples of an MK-40 cation-exchange membrane with the particle size of the ion exchanger of (a, b) <20 μm and (c, d) 56–71 μm at a magnification of ×500.

regions of the ion exchanger or macropore was meant to be the size of the ion-exchange resin particle or macropore. To assess the structural characteristics, four to five micrographs obtained for different regions of the surface of the membranes under study were analyzed.

RESULTS AND DISCUSSION

Structural and Physicochemical Properties of the Membranes

The electron micrographs of the surface and cross-section of the initially swelled samples of MK-40 and MA-41 heterogeneous membranes with different particle sizes of the ion exchanger are presented in Figs. 2 and 3. The visualization of the surface of different membranes has shown that the particle sizes of the ion-exchange resin are almost in the same range.

A comparison of the SEM images of the surface and cross-section of the initially swelled samples of the membranes has revealed a difference in the concentration and sizes of the particles of the ion-exchange resin for both cation- and anion-exchange membranes. An almost twofold increase in the fraction of the conductive phase in the section in comparison with the surface of the cation-exchange membrane has been found. This fact is associated with the ejection of plastic polyethylene from the bulk onto the surface in the process of fabrication of the membranes which leads to encapsulation of resin particles. Figure 4 shows the histograms of distribution of the fraction of ion-exchange resin particles with different radii of the total area of the conductive phase on the surface and in the section of the membrane with a particle size of 56–71 μm. It has been found that particles with a radius of 16 to 30 μm are absent on the surface but their fraction is 40% of the total area of the phase of the ion exchanger in the cross-section of the membrane.

A comparison of the histograms of distribution of the fraction of the ion-exchange resin particles with different radii from the total area of the conductive

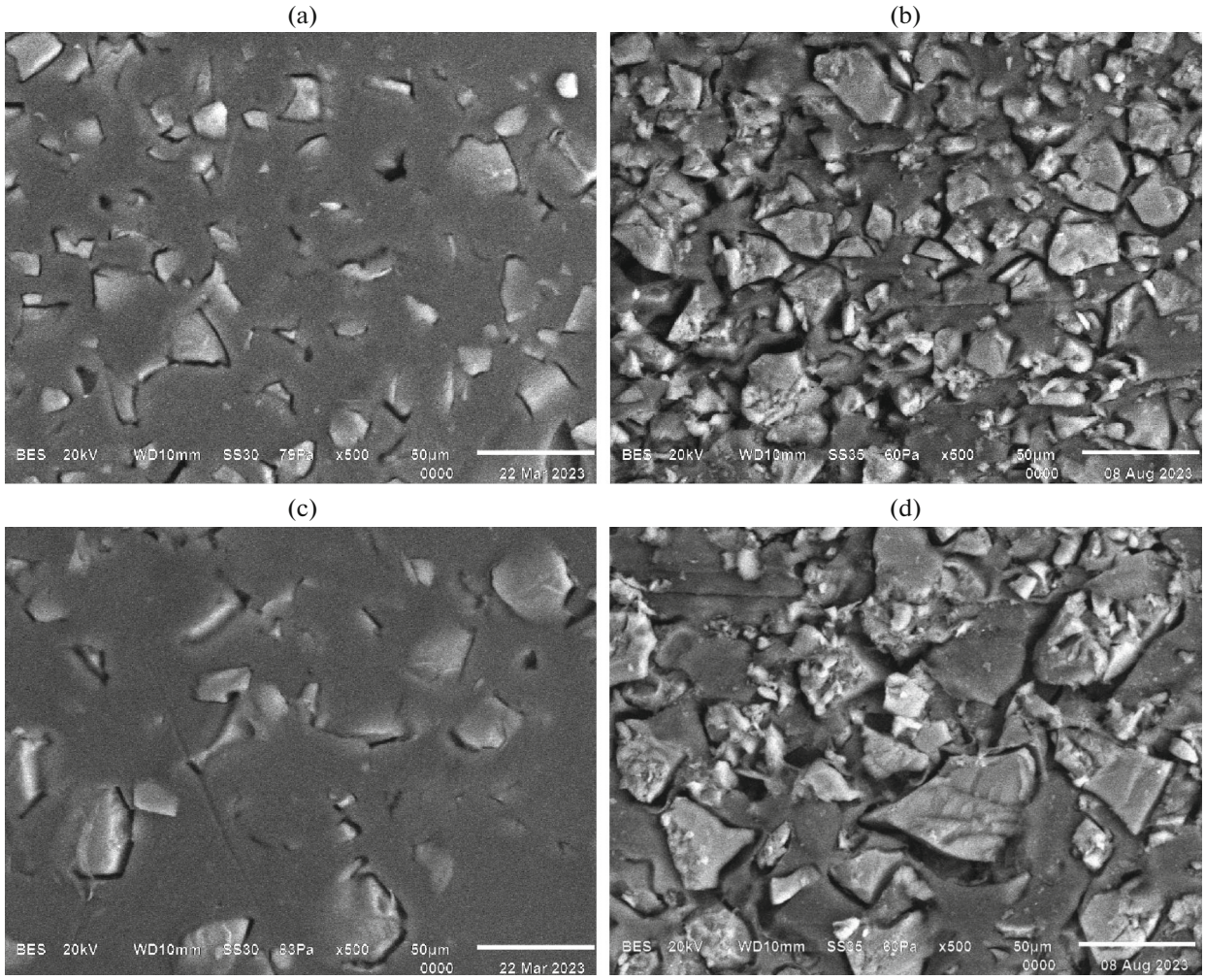

Fig. 3. SEM images of the (a, c) surface and (b, d) section of the initially swelled samples of an MA-41 anion-exchange membrane with the particle size of the ion exchanger of (a, b) <20 μm and (c, d) 56–71 μm at a magnification of ×500.

phase in the cross-section of the initially swelled membranes with the minimum and maximum size of the ion exchangers (Fig. 5) has revealed a quite significant difference in the structural characteristics of the section of the samples.

The presence of small particles in the samples of the membrane with a particle size of 56–71 μm is apparently associated with their adhesion to form larger agglomerates at the stage of grinding and passage through the sieves in such a form. Upon heating a mixture of polyethylene and a resin in the process of forge rolling of a blank and further pressing of a membrane, the agglomerates "disintegrate," which manifests itself in the appearance of small ion exchanger particles in the micrographs of the surface and section of the membranes.

With the decrease in the particle size of the ion-exchange resin, a growth in their exit onto the surface of the membranes and an increase in the number of macropores have been found (Table 1). The fraction of the ion exchanger on the surface of MK-40 and MA-41 membranes increases by 15 and 19%, and macroporosity, by 6 and 37%, respectively, in the case of a decrease in the particle size of the ion exchanger. Here, the value of the pore radius decreases by 22% for an MK-40 membrane and by 18%, for an MA-41 membrane.

For a section of the cation-exchange membrane with the maximum particle size of the ion-exchange resin, a fourfold increase in the macroporosity and a 1.5-fold increase in the pore size in comparison with the surface have been found.

The main physicochemical characteristics of MK-40 and MA-41 membranes with varied dispersity of the ion-exchange resin particles are presented in Table 2. In the studied samples, the concentration of the ion-exchange resin corresponds to that for commercially available membranes with polydisperse distribution of the particles of the ion exchanger. The exchange capacity Q of the membranes slightly

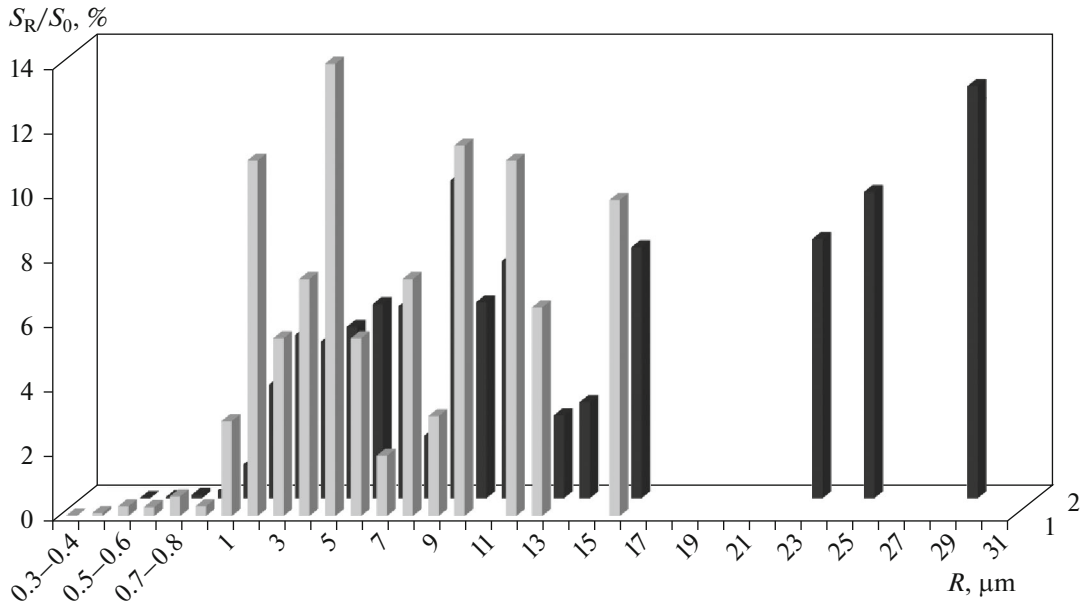

Fig. 4. Fraction of the ion-exchange resin particles with different radii S_R on the total area of the conductive phase S_0 (1) on the surface and (2) in the section of an MK-40 cation-exchange membrane with the particle size of the ion exchanger of 56–71 μm.

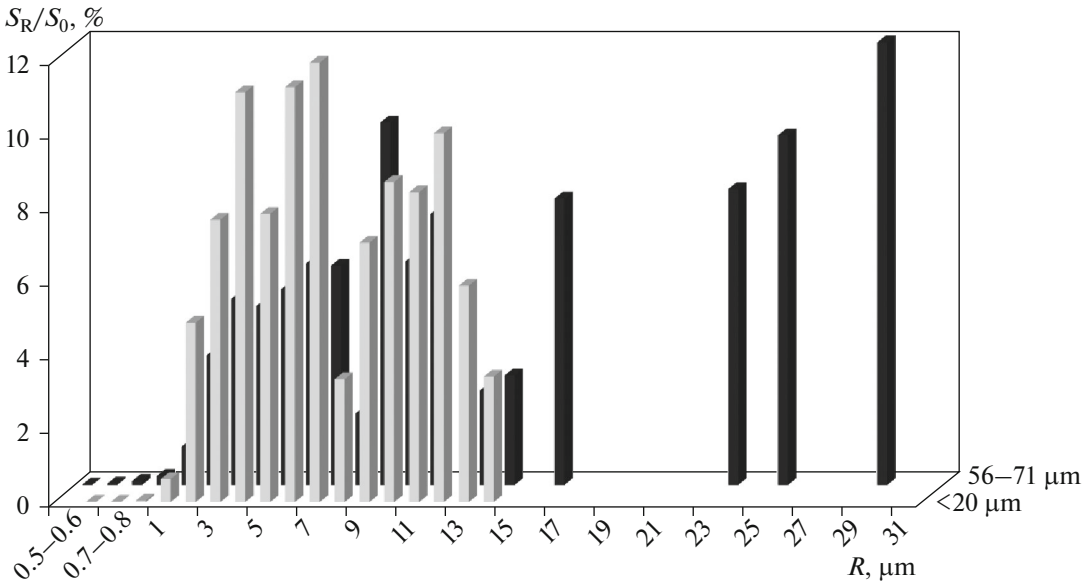

Fig. 5. Fraction of the ion-exchange resin particles with different radii S_R on the total area of the conductive phase S_0 in the section of samples of MK-40 membranes with different particle sizes of the ion exchanger.

changes as the particle size of the ion exchanger decreases, which corresponds to its identical concentration in the samples. The value of the exchange capacity of the cation-exchange membranes is 2.3-fold higher when compared to the anion-exchange membranes, which is determined by the higher exchange capacity of a KU-2-8 cation exchanger present in the composition of the membranes in comparison with an AV-17-8 anion exchanger. The water content W of the cation-exchange membranes has close values in a range of particle sizes of 20–71 μm and increases when the particle size is less than 20 μm. For the anion-exchange membranes, the value of W significantly increases with the decrease in the particle size of the ion exchanger. A similar regularity is observed for the specific water content n_m which formally describes the number of water molecules per one functional group.

Table 2. Main physicochemical characteristics of MK-40 and MA-41 membranes with varied dispersity of the ion-exchange resin particles

No.	Particle size of the ion-exchange resin, μm	Weight fraction of the ion-exchange resin, %	Q, $mmol/g_{sw}$	ρ, g/cm^3	W, %	n_m, $mol_{H_2O}/mol_{SO_3^-}$
MK-40 cation-exchange membranes						
1	56–71	65	1.35	1.160	35	14.3
2	40–56		1.38	1.167	33	13.3
3	32–40		1.37	1.156	34	13.9
4	20–32		1.36	1.159	34	14.0
5	<20		1.36	1.171	37	15.1
MA-41 anion-exchange membranes						
6	56–71	60	0.58	1.038	24	23.1
7	40–56		0.55	1.036	27	27.0
8	32–40		0.58	1.029	29	27.3
9	20–32		0.61	1.033	31	28.3
10	<20		0.63	1.036	39	34.5

The obtained dependences are in agreement with the changes in the values of the surface porosity of the membranes taking into account the structural defects determined based on the SEM images. As is seen from Table 1, the concentration of the ion-exchange resin on the surface of the cation-exchange membrane is higher in comparison with the anion-exchange membrane, which correlates with its higher weight fraction introduced at the stage of fabrication and is in agreement with the results of [21].

Specific Conductivity of the Membranes

The concentration dependences of the specific conductivity of the studied membranes in solutions of sodium chloride are presented in Fig. 6. It has been found that the electrical conductivity of the samples of cation-exchange membranes (Fig. 6a) is overall higher when compared to anion-exchange membranes (Fig. 6b). The electrical conductivity of the membranes grows with the decrease in the particle size of the resin, which is determined by the increase in the water content of the samples. However, specific conductivities of MK-40 cation-exchange membranes with the particle sizes of the ion-exchange resin of 56–71 and <20 μm significantly differ. The curves for the samples of the membranes with the particle size in ranges of 40–56, 32–40, and 20–32 μm coincide within the limits of error of determination. It has been found that the dispersity of the ion-exchange resin particles more affects the conductivity of the samples of anion-exchange membranes. A reason for the different behavior of cation- and anion-exchange membranes may be different concentration of fixed groups Q in them, which leads to a more substantial effect of the internal solution phase on the conductivity of the samples.

Diffusion Permeability of the Samples of Membranes

Figure 7 presents the concentration dependences of the integral coefficients of diffusion permeability of the membranes in solutions of sodium chloride. The analysis of the obtained dependences shows that, for the diffusion permeability of the membranes, regularities similar to those for their specific conductivity are observed. The diffusion permeability of the cation-exchange membranes is higher when compared to the samples of anion-exchange membranes due to the higher water content and porosity (Tables 1, 2). With the decrease in the particle size of the ion-exchange resin, the water content and diffusion permeability of the membranes grow. This effect is more pronounced for the samples of anion-exchange membranes. An exception from this dependence is the maximum throughout the entire range of concentrations value of diffusion permeability of an MA-41 anion-exchange membrane with the particle size of the ion exchanger of 20–32 μm. In addition, varying the particle sizes of the resin from 71 to 40 μm does not lead to any significant change in diffusion permeability for both cation- and anion-exchange membranes. The measured values of permeability for these samples coincide within the limits of error of determination.

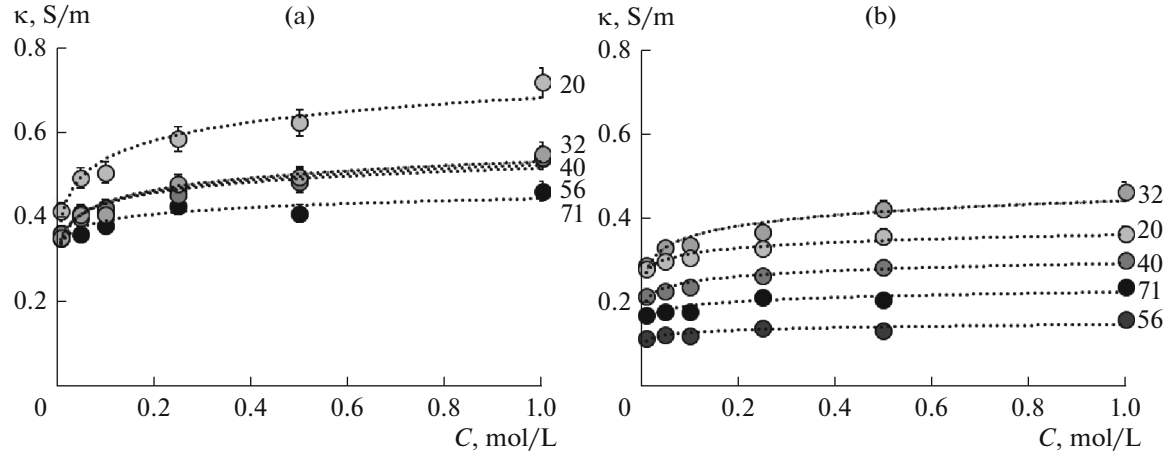

Fig. 6. Concentration dependences of the specific conductivity of (a) MK-40 and (b) MA-41 membranes in solutions of sodium chloride. The numbers at the curves correspond to the largest particle size in the fraction.

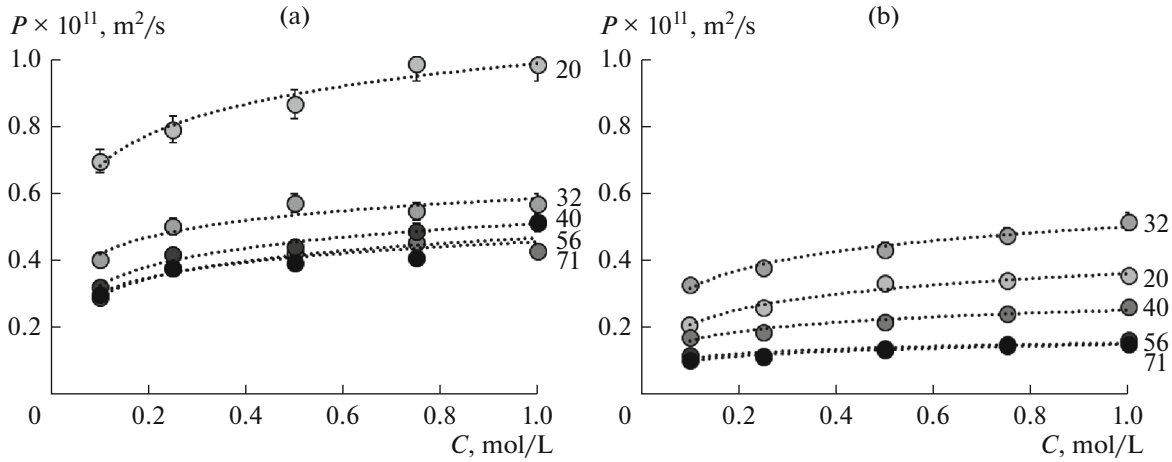

Fig. 7. Concentration dependences of the integral coefficients of diffusion permeability of (a) MK-40 and (b) MA-41 membranes in solutions of sodium chloride. The numbers at the curves correspond to the largest particle size in the fraction.

Results of the Assessment of the Transport-Structural Parameters of the Membranes

The transport-structural parameters of a microheterogeneous model calculated based on the experimental dependences of specific conductivity (Fig. 6) and diffusion permeability (Fig. 7) are presented in Table 3. It has been found that varying the particle sizes of the cation exchanger in MK-40 membranes leads to a change in the values of the model parameters. The volume fraction of the gel phase (the parameter f_1) decreases with the decrease in the particle size of the cation exchanger by 8%. Here, the value of the parameter f_2 that characterizes the volume fraction of the intergel solution phase increases more than twofold. The values of the parameter α that characterizes the arrangement of the gel and internal solution phases change by 15%.

The analysis of the values of conductivity of the gel phase of the membrane κ_{iso} has shown that an increase in the conductivity of the gel phase is observed with a decrease in the particle size of the ion exchanger in the samples of MA-41 anion-exchange membranes. A probable reason is the increase in the hydrate capacity of the gel phase with the decrease in the particle size of the ion exchanger despite the increase in the fraction of the intergel solution. This leads to an increase in the mobility of counterions in the gel which can also be affected by the increase in the accessibility of the ion-exchange groups for transfer. Due to the same reason, the parameter G that characterizes the transport of coions in the gel phase also increases. For cation-exchange membranes, the specified effects manifest themselves only in the case of a sample with a particle size below 20 μm.

Table 3. Transport-structural parameters of MK-40 and MA-41 heterogeneous membranes with varied dispersity of the ion-exchange resin particles calculated by the microheterogeneous model

No.	Particle size, μm	κ_{iso}, S/m	$G \times 10^{16}$, $m^5\ mol^{-1}\ s^{-1}$	f_1	α
MK-40 cation-exchange membranes					
1	56–71	0.39	2.69	0.94	0.44
2	40–56	0.38	1.94	0.90	0.37
3	32–40	0.39	1.57	0.91	0.38
4	20–32	0.39	1.18	0.89	0.38
5	<20	0.47	1.69	0.87	0.38
MA-41 anion-exchange membranes					
6	56–71	0.15	0.19	0.90	0.30
7	40–56	0.10	0.13	0.91	0.33
8	32–40	0.20	0.45	0.89	0.32
9	20–32	0.29	1.16	0.87	0.32
10	<20	0.26	1.85	0.90	0.34

Table 4. Transport-structural parameters of MK-40 and MA-41 membranes with varied dispersity of the ion-exchange resin particles calculated by the extended three-wire model

No.	Particle size, μm	*a*	*b*	*c*	*d*	*e*
MK-40 cation-exchange membranes						
1	56–71	0.055	0.94	0.0088	0.38	0.62
2	40–56	0.19	0.80	0.011	0.50	0.50
3	32–40	0.14	0.85	0.0084	0.48	0.52
4	20–32	0.19	0.80	0.011	0.50	0.50
5	<20	0.21	0.77	0.014	0.50	0.50
MA-41 anion-exchange membranes						
6	56–71	0.13	0.86	0.0065	0.49	0.51
7	40–56	0.16	0.84	0.0038	0.53	0.47
8	32–40	0.12	0.87	0.0071	0.48	0.52
9	20–32	0.16	0.83	0.013	0.48	0.52
10	<20	0.19	0.80	0.0073	0.52	0.48

The results of the calculation of the transport-structural parameters of the extended three-wire model by the concentration dependences of specific conductivity are presented in Table 4. Overall, general regularities in the change of the current flow paths upon varying the particle size of the ion exchanger are observed for both series of membranes. In the case of decreasing the particle size of the ion exchanger, a decrease in the contribution from the transfer along the gel channel (the parameter *b*) and an increase in the current transfer along the mixed channel (the parameter *a*) and solution channel (the parameter *c*) have been found.

The results of independent studies of the surface and section of the membranes by SEM are in agreement with the change in the model parameters and confirm the correlation between the conductive properties and structural changes in MK-40 and MA-41 membranes upon varying the particle size of the ion exchanger in them.

The obtained values of the parameter *c* were used for the calculation of the transfer numbers of counterions through the membranes by formula (4). The concentration dependences of the transfer numbers of counterions in the studied membranes are presented in Fig. 8. It has been shown that, despite the structural

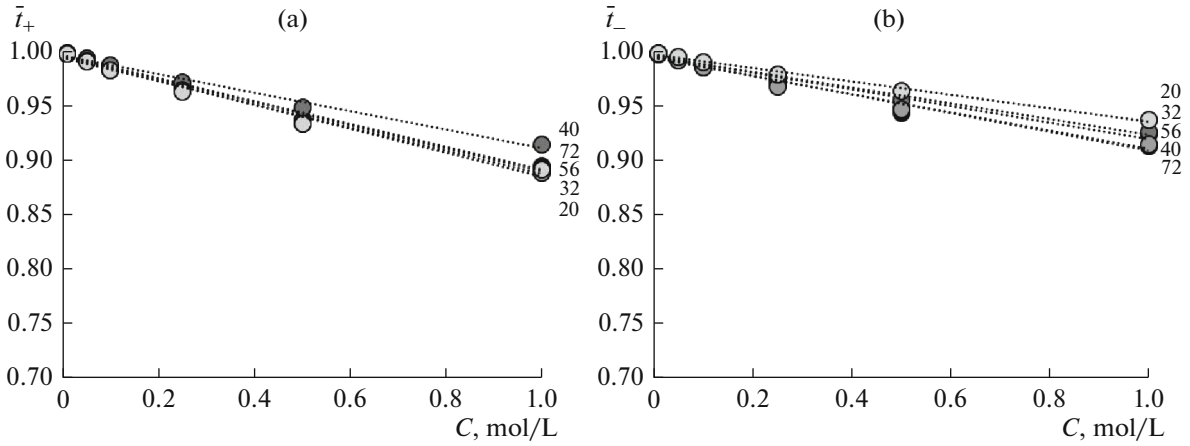

Fig. 8. Concentration dependences of the transfer numbers of counterions in the (a) cation- and (b) anion-exchange membranes with different particle sizes of the ion-exchange resin.

reorganization, the samples of all the membranes retain high values of selectivity in solutions of sodium chloride with a concentration of up to 1 M.

CONCLUSIONS

The structural, physicochemical, and transport characteristics of experimental MK-40 and MA-41 heterogeneous ion-exchange membranes with varied dispersity of the ion-exchange resin particles have been measured. The studies of the structural characteristics have shown that the membranes have a clearly pronounced anisotropic morphology of the surface and section which is determined by the effect of encapsulation of the ion-exchange resin particles by polyethylene on the surface in the process of production. For the cation-exchange membrane with the maximum particle size of the ion exchanger, large resin particles with a radius over 16 μm have only been detected on the section and are over 40% of the total area of the ion exchanger phase. The internal phase of the membrane is also characterized by higher macroporosity and pore size. A fourfold decrease in macroporosity and a 1.5-fold decrease in the weighted average pore size have been found on the surface in comparison with the internal phase. In the case of decreasing the particle sizes of the cation-exchange resin down to <20 μm, an increase in the surface macroporosity by 6–10% has been found.

The exchange capacity of the samples of experimental membranes slightly changes upon varying the particle size of the ion exchanger. Here, it has been found that the exchange capacity of the cation-exchange membranes exceeds the corresponding values for the anion-exchange membranes more than twofold. The water content of the anion-exchange membranes increases with the decrease in the particle size of the ion exchanger and increase in the macroporosity. The water content of the cation-exchange membranes is significantly higher only for a sample with the particle size of the resin of less than 20 μm.

The analysis of the concentration dependences of the specific conductivity and diffusion permeability of the membranes in solutions of sodium chloride has shown that a decrease in the particle size of the resin in the composition of MK-40 cation-exchange membranes in a range of 71 to 20 μm does not significantly affect the transport characteristics. Further decreasing the particle size down to <20 μm leads to a growth in the values of specific conductivity by 30% and diffusion permeability more than twofold. A more significant growth in the transport characteristics is observed for MA-41 anion-exchange membranes. The values of specific conductivity and diffusion permeability in 1 M solution of sodium chloride increase twofold and 3.5-fold in the case of decreasing the particle size of the anion exchanger from 71 down to 20 μm, respectively.

Based on the concentration dependences of the transport characteristics of the experimental membranes, the transport-structural parameters of the microheterogeneous and extended three-wire models have been calculated. The analysis of the values of the model parameters has shown that, in the case of decreasing the particle size of the ion-exchange resin, an increase in the conductivity of the gel phase of the membrane is observed as well as redistribution of the current transfer paths in the membrane occurs. It has been found that the reorganization of the current transfer paths leads to an increase in the contribution from the transfer along the equilibrium solution channel, which is in agreement with the increase in their water content and macroporosity. It should also be noted that the found changes in the transport-structural parameters of the cation- and anion-exchange membranes do not lead to any substantial change in selectivity.

ACKNOWLEDGMENTS

The results of the studies were partially obtained on the equipment of the Center for Collective Use of the Voronezh State University. URL: https://ckp.vsu.ru.

FUNDING

The study was supported by a grant from the Russian Science Foundation no. 21-19-00397, https://rscf.ru/en/project/21-19-00397/.

CONFLICT OF INTEREST

The authors of this work declare that they have no conflicts of interest.

REFERENCES

1. E. M. Akberova and V. I. Vasil'eva, Electrochem. Commun. **111**, 106659 (2020).
2. P. V. Vyas, P. Ray, S. K. Adhikary, B. G. Shah, and R. Rangarajan, J. Colloid Interface Sci. **257**, 127 (2003).
3. J. Balster, M. H. Yildirim, D. F. Stamatialis, R. Ibanez, R. G. H. Lammertink, V. Jordan, and M. Wessling, J. Phys. Chem. B **111**, 2152.
4. S. M. Davidson, M. Wessling, and A. Mani, Sci. Rep. **6**, 22505 (2016).
5. J. H. Choi, S. H. Kim, and S. H. Moon, J. Colloid Interface Sci. **241**, 120 (2001).
6. S. M. Hosseini, S. S. Madaeni, and A. R. Khodabakhshi, J. Membr. Sci. **351**, 178 (2010).
7. S. M. Hosseini, S. S. Madaeni, A. R. Heidari, and A. R. Moghadassi, Desalination **279**, 306 (2011).
8. S. M. Hosseini, S. S. Madaeni, A. R. Heidari, and A. R. Khodabakhshi, Desalination **285**, 253 (2012).
9. A. E. Mofrad, A. Moheb, M. Masigol, M. Sadeghi, and F. Radmanesh, J. Colloid Interface Sci. **532**, 546 (2018).
10. B. Wang, M. Wang, K. Wang, and Yu. Jia, Desalination **384**, 43 (2016).
11. V. I. Vasil'eva, A. V. Zhiltsova, E. M. Akberova, and A. I. Fataeva, Kondens. Sred. Mezhfaz. Gran. **16**, 257 (2014).
12. P. V. Vyas, B. G. Shah, G. S. Trivedi, P. Ray, S. K. Adhikary, and R. Rangarajan, React. Funct. Polym. **44**, 101 (2000).
13. P. V. Vyas, B. G. Shah, G. S. Trivedi, P. Ray, S. K. Adhikary, and R. Rangarajan, J. Membr. Sci. **187**, 39 (2001).
14. N. P. Berezina, S. V. Timofeev, and N. A. Kononenko, J. Membr. Sci. **209**, 509 (2002).
15. L. V. Karpenko, O. A. Demina, G. A. Dvorkina, S. B. Parshikov, C. Larchet, B. Auclair, and N. P. Berezina, Russ. J. Electrochem. **37**, 287 (2001).
16. O. A. Demina, N. A. Kononenko, and I. V. Falina, Pet. Chem. **54**, 515 (2014).
17. V. I. Zabolotsky and V. V. Nikonenko, J. Membr. Sci. **79**, 181 (1993).
18. N. P. Berezina, N. A. Kononenko, O. A. Dyomina, and N. P. Gnusin, Adv. Colloid Interface Sci. **139**, 3 (2008).
19. S. Dzh. B. Rid, *Electron Probe Microanalysis and Scanning Electron Microscopy in Geology* (Tekhnosfera, Moscow, 2008) [in Russian].
20. V. I. Vasil'eva, E. M. Akberova, A. V. Zhiltsova, E. I. Chernykh, E. A. Sirota, and B. L. Agapov, J. Surf. Investig. X-ray, Synchrotron Neutron Tech. **7**, 833 (2013).
21. L. Vobecká, M. Svoboda, J. Beneš, T. Belloň, and Z. Slouka, J. Membr. Sci. **559**, 127 (2018).

Translated by E. Boltukhina